Mutually unbiased bases in six dimensions: The four most distant bases

Philippe Raynal,[1] Xin Lü,[1,2] and Berthold-Georg Englert[1,2]
[1]*Centre for Quantum Technologies, National University of Singapore, 3 Science Drive 2, 117543, Singapore*
[2]*Department of Physics, National University of Singapore, 2 Science Drive 3, 117542, Singapore*
(Received 5 March 2011; published 6 June 2011)

We consider the average distance between four bases in six dimensions. The distance between two orthonormal bases vanishes when the bases are the same, and the distance reaches its maximal value of unity when the bases are unbiased. We perform a numerical search for the maximum average distance and find it to be strictly smaller than unity. This is strong evidence that no four mutually unbiased bases exist in six dimensions. We also provide a two-parameter family of three bases which, together with the canonical basis, reach the numerically found maximum of the average distance, and we conduct a detailed study of the structure of the extremal set of bases.

DOI: 10.1103/PhysRevA.83.062303 PACS number(s): 03.67.−a, 03.65.Ta

I. INTRODUCTION

Two orthonormal bases of a Hilbert space are said to be unbiased if the transition probability from any state of the first basis to any state of the second basis is independent of the two chosen states. In the finite dimensional case of $\mathbb{C}^d$, the normalization of the two basis states $|a_i\rangle$ and $|b_j\rangle$ of two unbiased bases implies the defining property

$$|\langle a_i|b_j\rangle|^2 = \frac{1}{d} \quad \text{for all} \quad i,j = 1,2,\ldots,d. \tag{1}$$

This maximum degree of incompatibility between two bases [1,2] states that the corresponding nondegenerate observables are complementary. Indeed, the technical formulation of Bohr's principle of complementarity [3] that is given in Ref. [4] relies on the unbiasedness of the pair of bases. Textbook discussions of this matter can be found in Refs. [5,6], and Ref. [7] is a recent review on mutually unbiased bases (MUB), which are sets of bases that are pairwise unbiased.

In addition to playing a central role in quantum kinematics, we note that MUB are important for quantum state tomography [8,9], for quantifying wave-particle duality in multipath interferometers [10], and for various tasks in the area of quantum information, such as quantum key distribution [11] or quantum teleportation and dense coding [12–14]. In the context of quantum state tomography, $d+1$ von Neumann measurements provide $d-1$ independent data, each in the form of d probabilities with unit sum, so that in total one has the required d^2-1 real numbers that characterize the quantum state. A set of $d+1$ MUB is optimal, in a certain sense [9], for these measurements—if there is such a set. Such a set is termed *maximal*; there cannot be more than $d+1$ MUB, since there are at most $d+1$ $(d-1)$-dimensional orthogonal subspaces in a (d^2-1)-dimensional real vector space [9].

Ivanovic [8] gave a first construction of maximal sets of MUB if the dimension d is a prime, and Wootters and Fields [9] succeeded in constructing maximal sets when d is the power of a prime. These two cases have been rederived in various ways; see Refs. [15–17], for example. For other finite values of d, maximal sets of MUB are unknown, but it is always possible to have at least three MUB (see [7] and references therein).

The smallest non-prime-power dimension is $d=6$. Little is known for sure about the six-dimensional case, for which Zauner has conjectured that no more than three MUB exist [18]. Numerical studies seem to support Zauner's conjecture [19,20]. Computer-aided analytical methods, such as Gröbner bases or semidefinite programming, have also been applied to this problem [21], but limitations in computational power have so far prevented any definitive answer.

Recently, Bengtsson *et al.* [22] introduced a distance between two bases for a quantification of the notion of "unbiasedness." The distance vanishes when the two bases are identical and attains its maximal value of unity when they are unbiased. One can then consider the average squared distance (ASD) between several bases and search for its maximal value. Importantly, this ASD is unity if the bases are pairwise unbiased, and only then. A numerical search for the maximum of the ASD between four bases in six dimensions can be performed. Actually, a numerical study on essentially the same quantity was recently carried out by Butterley and Hall [23]. In terms of the ASD, they found the surprisingly large but strictly less-than-one maximal value of 0.9983. This is strong evidence that no more than three MUB exist in six dimensions. However, the set of bases behind this maximum value is not reported in Ref. [23].

It is the objective of the present paper to close this gap. In Sec. II we review the notion of Bengtsson *et al.* for the distance between bases. We perform a numerical search for the maximum ASD between four bases in six dimensions and report, in Sec. III, our results which confirm the maximum found by Butterley and Hall. We then provide a two-parameter family of three bases which, together with the canonical basis, reaches the numerically found maximum, for which we give a closed expression. We study this family in detail in Sec. IV and conclude with a summary and outlook. Some matters of a technical nature are reported in the appendixes.

II. DISTANCE BETWEEN BASES

The main goal of this paper is twofold. First we numerically search for the maximum value of the ASD between four bases in six dimensions and see that we cannot obtain four MUB. And second, we provide a two-parameter family of three bases which, together with the canonical basis, reaches the numerically found maximum.

Following Bengtsson *et al.* [22], we consider two orthonormal bases of kets of $\mathbb{C}^d$, $a = \{|a_i\rangle\}$ and $b = \{|b_j\rangle\}$, and quantify their squared distance by

$$D_{ab}^2 = 1 - \frac{1}{d-1}\sum_{i,j=1}^{d}\left(|\langle a_i|b_j\rangle|^2 - \frac{1}{d}\right)^2$$
$$= \frac{1}{d-1}\sum_{i,j=1}^{d}|\langle a_i|b_j\rangle|^2(1-|\langle a_i|b_j\rangle|^2)\,. \qquad (2)$$

Clearly, this distance is symmetrical, $D_{ab} = D_{ba}$ and vanishes when the bases are the same, that is, when the two sets of projectors $\{|a_i\rangle\langle a_i|\}$ and $\{|b_j\rangle\langle b_j|\}$ are identical; the maximal distance is unity, $D_{ab} \leqslant 1$; and this maximum is reached if the bases are unbiased, $|\langle a_i|b_j\rangle|^2 = 1/d$, and only then.

In the original reasoning by Bengtsson *et al.*, D_{ab} is actually the chordal Grassmanian distance of two planes in the (d^2-1)-dimensional real vector space associated with traceless Hermitian operators in the d-dimensional complex Hilbert space. One can also view D_{ab} as the Hilbert-Schmidt distance between two rank-d statistical operators in $\mathbb{C}^d \otimes \mathbb{C}^d$ that are in one-to-one correspondence with the d-dimensional bases. Consult Appendix A for this matter.

For a set of k bases, we have the ASD between the $k(k-1)/2$ pairs of bases, given by

$$\overline{D^2} = \frac{2}{k(k-1)}\sum_{a<b=1}^{k} D_{ab}^2\,. \qquad (3)$$

Owing to the normalization, we have $\overline{D^2} \leqslant 1$, with $\overline{D^2} = 1$ only if the k bases are pairwise unbiased.

With this notion of distance at hand, we can numerically search for the maximum ASD between four bases in six dimensions and see whether we obtain $\overline{D^2} = 1$, or in other words, if we can find four MUB. This search is the subject matter of the next section.

III. NUMERICAL STUDY

Our numerical approach relies on the mapping between one-qudit operators and two-qudit states established in Chapter 3 of Ref. [7]. Plus we use the steepest-ascent algorithm to find the maximum ASD between four bases in six dimensions. Details of the numerical method are presented in Appendix A. Our numerical results are reported below.

A similar numerical study was recently performed by Butterley and Hall [23] who minimized $1 - \overline{D^2}$ with the so-called Levenberg-Marquardt algorithm. Our approach confirms the extremal value they found, and we also exhibit the structure of the four bases that maximize $\overline{D^2}$ for $d = 6$.

We have used our code not only in dimension $d = 6$ but also for other d values as a means of benchmarking. We have run our code 2 500 times for two to five dimensions, 10 000 times for six dimensions, and 300 times for seven dimensions, both for $k = d + 1$ bases and for four bases. Our results are summarized in Table I.

Only in two cases, the maximum ASD does not reach the upper bound of $\overline{D^2} = 1$. They are the cases of four bases in two and six dimensions.

TABLE I. Rate of success and CPU time for the steepest-ascent search for the maximum ASD. The absolute maximum of $\overline{D^2} = 1$ is always reached for $d + 1$ bases in dimensions $d = 2$, 3, 4, and 5. As the seven-dimensional case illustrates, the difficulty of finding the global maximum increases rapidly with the dimension because there are many local maxima at which the steepest-ascent search can get stuck. We have also looked for the largest ASD between four bases in two to seven dimensions. We could not find four MUB in two or six dimensions. The CPU time refers to a Intel®Core™2 Duo CPU E6550 processor at 2.33 GHz, supported by 3.25 GB of RAM.

	$d+1$ bases			4 bases		
d	$\overline{D^2}_{\max}$	Success rate (%)	CPU time (s)	$\overline{D^2}_{\max}$	Success rate (%)	CPU time (s)
2	1	100	0.049	8/9	100	0.108
3	1	99.9	0.272	1	99.9	0.272
4	1	100	1.268	1	100	0.976
5	1	99.7	4.432	1	59.8	10.995
6	0.9849	39.2	188.407	0.9983	69.6	20.158
7	1	3.8	467.157	1	1.1	101.002

At most, three MUB can be constructed in two dimensions. Thus the maximum ASD between four bases has to be less than unity. This example is interesting because it can be analytically solved. In $\mathbb{R}^3$, the four bases correspond to the tetrahedron, where each edge represents a basis.

Importantly, we have searched for the maximum ASD between four bases in six dimensions. We have found the largest value to be $\overline{D^2}_{\max} = 0.9983$. In the search for the global maximum, we have also found a few other local maxima whose frequencies of occurrence are reported in Fig. 1. These results are consistent with those reported by Butterley and Hall [23]. We find the same local and global maxima with very similar frequencies. This is as expected because we have generated the four random bases from which the search proceeds in the same

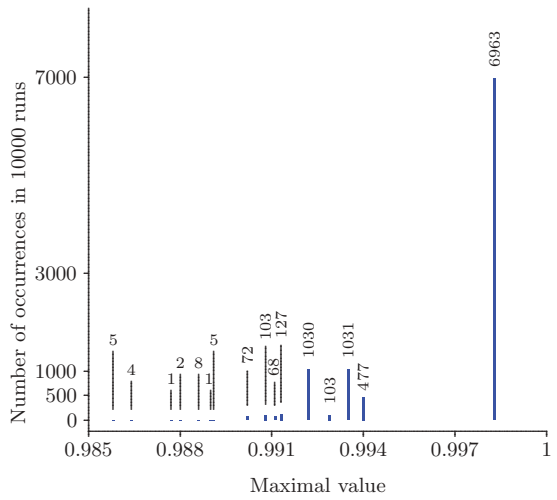

FIG. 1. (Color online) Histogram of the maximum values of the ASD found during a numerical search for 10 000 randomly chosen initial four bases. The search converges to one of the local maxima in about 30% of all runs, and to the global maximum of $\overline{D^2}_{\max} = 0.9983$ for the other 70% of initial bases.

way as Butterley and Hall, using the same dedicated Matlab command. The two numerical methods are different, however. We use the steepest-ascent algorithm while they employ the Levenberg-Marquardt algorithm for a nonlinear least-squares optimization.

Since we consider four bases, there are six pairs of bases, and their respective distances are not without interest. Indeed, it turns out that one basis is unbiased with the three remaining bases. And these three remaining bases are themselves equidistant. The immediate implication is that the privileged basis can be chosen to be the computational basis, while the three remaining bases are Hadamard bases; that is, the unitary matrices composed of the columns that represent the basis kets with reference to the computational basis are complex Hadamard matrices divided by $\sqrt{6}$. We recall here that a complex Hadamard matrix is a d-dimensional square matrix satisfying the two conditions of unimodularity and orthogonality [24]

$$\begin{aligned} &|H_{ij}| = 1 \quad \text{for } i,j = 1,\ldots,d\,, \\ &H H^\dagger = d\mathbb{1}\,. \end{aligned} \tag{4}$$

Therefore, the unitary matrix $H/\sqrt{d}$ has matrix elements that can be related to a pair of unbiased bases: $\langle a_i|b_j\rangle = H_{ij}/\sqrt{d}$.

In addition to maximizing $\overline{D^2}$, our code also returns the four bases for which the maximum is achieved. After a bit of polishing—the set of four bases is not unique, since global unitary transformations yield equivalent sets, and the order of kets in each basis is arbitrary—this allows us to seek for the structure hidden behind the maximum ASD. In the next section we will present a two-parameter family of three bases. The two parameters are two phases, while the three bases are three Hadamard bases. We study in detail the properties of this family and show that, for some definite values of the two parameters, these three bases together with the canonical basis reach the numerically found maximum ASD of 0.9983. This definite structure of the optimal four bases is our main result, with a closed expression for $\overline{D^2}_{\max}$ as a most welcome bonus; see Eq. (22) below.

Harking back to Table I, we note that the best set of seven bases in six dimensions has an ASD of 0.9849, short of unity by a mere one-and-a-half percent. For all practical purposes—those of state tomography, say—these seven bases are marginally worse than the imaginary seven MUB that no one has managed to find.

IV. THE TWO-PARAMETER FAMILY

Following Karlsson [25], we express the two-parameter family in terms of 2×2 block matrices where each of the nine blocks is itself a complex Hadamard matrix. Such 2×2 block matrices are called H_2 reducible. The two-parameter family contains three bases, the fourth basis being the canonical basis. We will see that these three Hadamard bases are equidistant, that their determinants are identical, and that they belong to the so-called Fourier transposed family F_6^T. Finally, we will show that together with the canonical basis they reach the numerically found maximum of the ASD.

A. Parametrization

We begin by defining a few quantities. We will need the third root of unity $\omega = \exp(i\,2\pi/3)$ as well as the following 2×2 matrices:

$$Z = \begin{bmatrix} 1 & 0 \\ 0 & -1 \end{bmatrix}, \quad X = \begin{bmatrix} x^* & 0 \\ 0 & x \end{bmatrix}, \quad F_2 = \begin{bmatrix} 1 & 1 \\ 1 & -1 \end{bmatrix},$$

and

$$T = \begin{bmatrix} 1 & \omega t^2 \\ 1 & -\omega t^2 \end{bmatrix}, \tag{5}$$

where $t = \exp(i\theta_t)$ and $x = \exp(i\theta_x)$ are two phases. Let us notice that T and F_2 are themselves Hadamard matrices.

The Hadamard matrices for the three bases are given by

$$\begin{aligned} M_1 &= \begin{bmatrix} X & 0 & 0 \\ 0 & i\omega^* t Z X^{*2} & 0 \\ 0 & 0 & X \end{bmatrix} \frac{1}{\sqrt{6}} \begin{bmatrix} F_2 & F_2 & F_2 \\ F_2 & \omega F_2 & \omega^* F_2 \\ T & \omega^* T & \omega T \end{bmatrix} \\ &= \frac{1}{\sqrt{6}} X_1 N_1\,, \\ M_2 &= \frac{1}{\sqrt{6}} \begin{bmatrix} F_2 & F_2 & F_2 \\ T & \omega T & \omega^* T \\ T & \omega^* T & \omega T \end{bmatrix} = \frac{1}{\sqrt{6}} N_2\,, \end{aligned}$$

and

$$\begin{aligned} M_3 &= \begin{bmatrix} X^* & 0 & 0 \\ 0 & \omega^* X^* & 0 \\ 0 & 0 & -it Z X^2 \end{bmatrix} \frac{1}{\sqrt{6}} \begin{bmatrix} F_2 & F_2 & F_2 \\ T & \omega T & \omega^* T \\ F_2 & \omega^* F_2 & \omega F_2 \end{bmatrix} \\ &= \frac{1}{\sqrt{6}} X_3 N_3\,. \end{aligned} \tag{6}$$

In the above parametrization, we have introduced the matrices X_i and N_i, $i = 1,2,3$, which we will address as dephasing and central matrices, respectively. The derivation of this parametrization is explained in Appendix B.

The next section is devoted to proving the three properties mentioned earlier. Before we turn to the proofs, we wish to point out that an additional relation between the two phases x and t exists,

$$\cos\left(\theta_t + \frac{1}{3}\pi\right) = \frac{\cos(2\theta_x)}{\sin(\theta_x)}\,. \tag{7}$$

It reduces the two-parameter family to a single-parameter family. Of course, as a subfamily, it conserves all the fundamental properties of the two-parameter family. Furthermore it still reaches the maximum ASD.

B. Properties

1. *Equidistance*

A significant property of the three proposed Hadamard matrices is their equidistance. The relevant terms that appear in the distance between the two bases M_a and M_b (i.e., $|\langle a_i|b_j\rangle|$) are the elements of the product matrix $M_a^\dagger M_b$ (i.e., $\langle a_i|b_j\rangle$) in absolute value. Therefore, if the three product matrices $M_1^\dagger M_2$, $M_2^\dagger M_3$, and $M_3^\dagger M_1$ have equal coefficients in absolute value,

then the three bases M_1, M_2, and M_3 are equidistant. This is exactly what happens here. Indeed, we have the following cyclic structure:

$$M_1^\dagger M_2 = \frac{1}{6}\begin{bmatrix} a_1 & a_2 & a_3 \\ a_3 & a_1 & a_2 \\ a_2 & a_3 & a_1 \end{bmatrix}, \quad M_2^\dagger M_3 = \frac{1}{6}\begin{bmatrix} b_1 & b_2 & b_3 \\ b_3 & b_1 & b_2 \\ b_2 & b_3 & b_1 \end{bmatrix},$$

and

$$M_3^\dagger M_1 = \frac{1}{6}\begin{bmatrix} c_1 & c_2 & c_3 \\ c_3 & c_1 & c_2 \\ c_2 & c_3 & c_1 \end{bmatrix}, \tag{8}$$

where, on the one hand, the 2×2 submatrices a_1, b_2, and c_3 have the same coefficients in absolute value and, on the other hand, a_2, a_3, b_1, b_3, c_1, and c_2 have the same coefficients in absolute value. More precisely, these matrices have the following forms (where the symbol $\check{}$ stands for swapping the two diagonal elements). First,

$$a_1 = \begin{bmatrix} \alpha & \beta \\ -\beta^* & \alpha^* \end{bmatrix}, \quad b_2 = \check{a}_1\,,$$

and

$$c_3 = \begin{bmatrix} i\omega t^*\beta & i\omega^* t\alpha \\ i\omega t^*\alpha^* & i\omega t^*\beta \end{bmatrix}. \tag{9}$$

Second,

$$a_2 = \begin{bmatrix} \gamma & \delta \\ \epsilon & \omega^*\gamma^* \end{bmatrix}, \qquad b_1 = \check{a}_2\,,$$

$$a_3 = \begin{bmatrix} \omega\gamma & -\epsilon^* \\ -\delta^* & \gamma^* \end{bmatrix}, \qquad b_3 = \check{a}_3\,, \tag{10}$$

$$c_1 = \begin{bmatrix} it^*\delta & i\omega t\gamma \\ i\omega^* t^*\gamma^* & -i\omega^* t^*\epsilon^* \end{bmatrix}, \quad c_2 = \check{c}_1\,.$$

The various coefficients in Eqs. (9) and (10) can be expressed in terms of the two angles θ_x and θ_t,

$$\begin{aligned} \alpha &= 4\cos(\theta_x)[1 - \omega t^* \sin(\theta_x)]\,, \\ \beta &= -2i\omega^* t[\cos(2\theta_x) - 2\cos(\theta_t - 2\pi/3)\sin(\theta_x)]\,, \\ \gamma &= -2\omega^* \cos(\theta_x)[\omega^* + 2t^* \sin(\theta_x)]\,, \\ \delta &= -2it[\cos(2\theta_x) - 2\cos(\theta_t)\sin(\theta_x)]\,, \\ \epsilon &= -2i\omega^* t^*[\cos(2\theta_x) - 2\cos(\theta_t + 2\pi/3)\sin(\theta_x)]\,. \end{aligned} \tag{11}$$

When Eq. (7) is fulfilled, we have $\epsilon = \omega^*\delta^*$ and a few simplifications arise. We obtain

$$a_3 = \omega Z a_2 Z\,, \quad b_3 = \omega Z b_1 Z\,, \quad \text{and } c_2 = -Z c_1 Z\,, \tag{12}$$

for example.

2. Determinant

A direct calculation shows that

$$\mathrm{Det}(X_1) = \mathrm{Det}(N_1) = \mathrm{Det}(X_3) = \mathrm{Det}(N_3) = wt^2\,. \tag{13}$$

Accordingly, the three Hadamard bases share the same determinant

$$\mathrm{Det}(M_1) = \mathrm{Det}(M_2) = \mathrm{Det}(M_3) = w^* t^4\,. \tag{14}$$

However, although the determinants are equal, there seems to be no simple relation between the three matrices M_1, M_2, and M_3. In particular, they do not have the same spectrum and are, therefore, not related by unitary operators.

3. Fourier transposed family

The Fourier transposed family, first studied by Haagerup [26], is parametrized by Karlsson in the form [25]

$$F_6^T \sim \begin{bmatrix} F_2 & F_2 & F_2 \\ T_1 & \omega T_1 & \omega^* T_1 \\ T_2 & \omega^* T_2 & \omega T_2 \end{bmatrix}, \tag{15}$$

where the 2×2 Hadamard matrices T_1 and T_2 are given by

$$T_i = \begin{bmatrix} 1 & t_i \\ 1 & -t_i \end{bmatrix}, \quad |t_i| = 1\,. \tag{16}$$

The equivalence relation in Eq. (15) means equality up to left and right dephasing and left and right permutations. In other words, the central matrix is the fundamental object that specifies the equivalence class. In the form of Eq. (6), it is clear that the three matrices N_1, N_2, and N_3 belong to the Fourier transposed family. As a result, the two-parameter family itself belongs to the Fourier transposed family.

Let us note here that only the right equivalence is natural for more than two bases, because it states that bases are defined up to permutations and global phases of their basis states. In particular, the distance between bases is invariant under right equivalence but not under left equivalence.

C. Average distance

Let us now compute the global maximum of the ASD between the three bases. Since the three bases are equidistant, we only have to compute the distance between, say, M_1 and M_2. A direct calculation leads to the following expression:

$$D_{12}^2(\theta_x,\theta_t) = \frac{8}{45}\left[5 - P\left(\sin(\theta_x), \cos\left(\theta_t + \frac{1}{3}\pi\right)\right)\right], \tag{17}$$

with the polynomial

$$\begin{aligned} P(p,q) = {} & 8p^8 + 8q^2p^6 - 16q^3p^5 + 16qp^5 - 16q^2p^4 \\ & + 8q^3p^3 - 7p^4 - 14qp^3 + 8q^2p^2 + 2p^2 + 4qp\,. \end{aligned} \tag{18}$$

We denote by $(p_{\mathrm{opt}},q_{\mathrm{opt}})$ the (p,q) pair for which $P(p,q)$ is minimal and, therefore, $D_{12}(\theta_x,\theta_t)$ is maximal. It turns out that q_{opt} is related to p_{opt} by

$$\cos\left(\theta_t^{\mathrm{opt}} + \frac{1}{3}\pi\right) = q_{\mathrm{opt}} = \frac{1 - 2p_{\mathrm{opt}}^2}{p_{\mathrm{opt}}}\,, \tag{19}$$

which is a particular evaluation of the function defined in Eq. (7), and p_{opt}^2 is the unique real solution of a cubic equation,

$$112p_{\mathrm{opt}}^6 - 192p_{\mathrm{opt}}^4 + 111p_{\mathrm{opt}}^2 = 22\,, \tag{20}$$

that is,

$$\sin\left(\theta_x^{\mathrm{opt}}\right)^2 = p_{\mathrm{opt}}^2 = \frac{3 + 16r - r^2}{28r} = 0.6946, \tag{21}$$

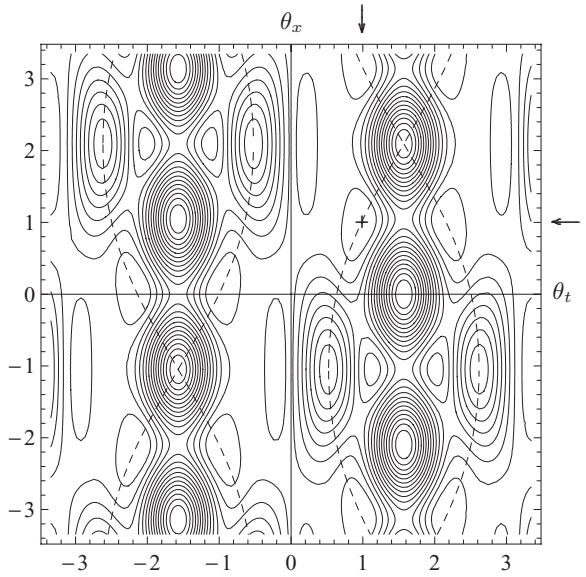

FIG. 2. Contour plot of the ASD for the two-parameter family. Along the dashed curves, relation (7) holds. The four single-parameter families—one for each dashed curve—are equivalent to the two-parameter family in the sense that the maximal and minimal value of the ASD can be found by searching along one of the dashed lines only. The arrows point to the location of one of the eight maxima at $(\theta_x,\theta_t) = (0.9852, 1.0094)$, marked by a cross.

with $r = (21\sqrt{3} - 36)^{1/3} = 0.7199$. It follows that there are eight optimal pairs of phases $(\theta_x^{\text{opt}},\theta_t^{\text{opt}})$ for which the maximal distance $D_{12}^{\max}$ is reached. The above expressions for θ_x^{opt} and θ_t^{opt} can be injected back into the formula of the distance to obtain first $D_{12}^{\max}$ and then

$$\begin{aligned}\overline{D^2}_{\max} &= \frac{1}{70}\left[71 - 12\cos\left(\theta_x^{\text{opt}}\right)^4\right] \\ &= \frac{1}{70}\left[71 - 3\left(\frac{r^2 + 12r - 3}{14r}\right)^2\right] = 0.9983, \end{aligned} \tag{22}$$

which agrees with the numerically found maximum ASD within the machine precision.

Furthermore, the distance D_{12} vanishes for

$$\begin{aligned} \theta_x &= \pi/2\,, \quad & \theta_t &= 0 \ (\text{mod}\ 2\pi/3), \\ \text{and}\ \ \theta_x &= -\pi/2\,, \quad & \theta_t &= \pi/3 \ (\text{mod}\ 2\pi/3)\,. \end{aligned} \tag{23}$$

As can be verified from the parametrization (6) or from the matrix products (8), the bases are indeed identical up to global phases and permutations for these values of the two phases θ_x and θ_t.

We can also consider the single-parameter family that we obtain when eliminating θ_t by using Eq. (7). Since Eq. (19) is equivalent to Eq. (7), this single-parameter family reaches the maximum of the ASD—and also the minimum, since Eq. (19) is obeyed by $(\theta_x,\theta_t) = (\pi/2, 2\pi/3)$. This is illustrated in Fig. 2, a contour plot of $\overline{D^2}$ for the two-parameter family of Hadamard bases, with the location of the (θ_x,θ_t) values of the single-parameter family indicated. The location of one of the eight maxima is marked, and the locations of the other seven follow from the symmetry properties of the contours.

V. SUMMARY AND OUTLOOK

We performed a numerical search for the maximum ASD between four bases in six dimensions. We found that it is strictly smaller than unity and so confirmed the recent study by Butterley and Hall [23]. We regard this result as strong evidence that no four MUB exist in six dimensions.

Next, we went beyond this numerical result by providing the four bases behind the numerically found maximum. More specifically, we found a two-parameter family of three bases, which together with the canonical basis, reaches the maximum of the ASD. We characterized this two-parameter family in full. We proved its inclusion in the Fourier transposed family and showed that the three bases are equidistant. Furthermore, we analytically computed the maximum ASD between these three Hadamard bases and the canonical basis to show that it reproduces the numerical result.

Two directions might be relevant for an extension of the present study. First, it would be interesting to see if the optimality of our solution can be extended to a larger family of bases, for example, to the whole Fourier transposed family. Second and complementarily, there might exist an argument to restrict the search for the maximum ASD between the canonical basis and three Hadamard bases to the Fourier transposed family, instead of the entire Hadamard family which, so far, has not been fully parametrized. In this context, however, it should be noted that—as follows from the findings of Jaming *et al.* [27]—there are no four MUB if one restricts the search to members of the Fourier family.

Finally, if there is no complete set of seven MUB in six dimensions, the optimal measurement for state tomography, in terms of statistical errors, remains to be found.

ACKNOWLEDGMENTS

Centre for Quantum Technologies is a Research Center of Excellence funded by the Ministry of Education and National Research Foundation of Singapore. The authors wish to express their grateful feelings to Ingemar Bengtsson for enlightening comments and friendly discussions.

APPENDIX A: NUMERICAL METHOD

As discussed in Sec. 3.1 of Ref. [7], for any ket $|\varphi\rangle$ or bra $\langle\phi|$ in a d-dimensional Hilbert space $\mathcal{H}$ or $\mathcal{H}^\dagger$, respectively, there is a conjugate bra or ket

$$\begin{aligned} \mathcal{H} \ni |\varphi\rangle &\longleftrightarrow \langle\varphi^*| \in \mathcal{H}^\dagger\,, \\ \mathcal{H}^\dagger \ni \langle\phi| &\longleftrightarrow |\phi^*\rangle \in \mathcal{H}, \end{aligned} \tag{A1}$$

such that

$$\langle\varphi^*|\phi^*\rangle = \langle\varphi|\phi\rangle^* = \langle\phi|\varphi\rangle\,. \tag{A2}$$

This mapping is not unique, but two different realizations differ at most by a unitary transformation. As a rule, $\langle\phi^*|$ and $\langle\phi| = |\phi\rangle^\dagger$ are different bras.

Once a particular choice of mapping has been made, there is a one-to-one correspondence between one-qudit operators and two-qudit kets,

$$|\varphi\rangle\langle\phi| \in B(\mathcal{H}) \longleftrightarrow |\phi^*,\varphi\rangle \in \mathcal{H}\otimes\mathcal{H}\,. \tag{A3}$$

In particular, for an orthonormal basis of kets in $\mathcal{H}$, $a = \{|a_1\rangle,|a_2\rangle\ldots,|a_d\rangle\}$, we have the conjugate basis $a^* = \{|a_1^*\rangle,|a_2^*\rangle,\ldots,|a_d^*\rangle\}$, and jointly they are used in defining the two-qubit state

$$\rho_a = \frac{1}{d}\sum_{j=1}^{d} |a_j^* a_j\rangle\langle a_j^* a_j|\,, \tag{A4}$$

which has the d-fold eigenvalue $1/d$ and the (d^2-d)-fold eigenvalue zero.

We normalize the Hilbert-Schmidt inner product of two-qudit operators in accordance with

$$(A,B) = d\,\mathrm{Tr}\{A^\dagger B\}\,, \tag{A5}$$

so that $(\rho_a,\rho_a) = 1$ and $(\rho_a,\rho_b) = 1/d$ for a pair of unbiased bases. For the two-qudit states associated with two single-qudit bases, we then have

$$(\rho_a,\rho_b) = \frac{1}{d}\sum_{j,k=1}^{d} |\langle a_j|b_k\rangle|^4 = 1 - \frac{d-1}{d}D_{ab}^2\,, \tag{A6}$$

with the distance D_{ab} of Eq. (2), where the identity $\langle a_j^* a_j|b_k^* b_k\rangle = |\langle a_j|b_k\rangle|^2$ is used. It follows that D_{ab} can be expressed in terms of the Hilbert-Schmidt norm of $\rho_a - \rho_b$,

$$D_{ab} = \sqrt{\frac{1}{2}\frac{d}{d-1}}\,\|\rho_a - \rho_b\|, \tag{A7}$$

with $\|A\| = \sqrt{(A,A)}$. This tells us something important: If $a \neq b$, then $\rho_a \neq \rho_b$, so that the mapping $a \leftrightarrow \rho_a$ is one-to-one.

In passing, we note the following challenge. Clearly, not all two-qudit states with $\rho = d\rho^2$ correspond to a single-qudit basis in the sense of Eq. (A4). But which additional criteria identify the set of two-qudit states that do?

We are interested in finding the maximum value of the ASD between k bases in dimension d. The numerical search begins with a randomly chosen initial set of bases, and then modifies the bases in each iteration round such that $\overline{D^2}$ is systematically increased.

An infinitesimal variation of a ket in basis a is given by

$$\delta|a_j\rangle = i\epsilon_a|a_j\rangle, \tag{A8}$$

where ϵ_a is an infinitesimal Hermitian operator acting on the basis a. We have one such Hermitian ϵ operator for each basis. The resulting response of $\overline{D^2}$ is

$$\delta\overline{D^2} = \sum_{a=1}^{k}\mathrm{tr}\{\epsilon_a G_a\}\,, \tag{A9}$$

where tr{ } is a single-qudit trace and

$$G_a = \frac{8}{k(k-1)(d-1)}\,\mathrm{Im}\left\{\sum_{b=1}^{k}\sum_{j,k=1}^{d}(|a_j\rangle\langle a_j|b_k\rangle\langle b_k|)^2\right\} \tag{A10}$$

is the ath component of the gradient. If bases a and b are unbiased, there is no contribution to G_a from basis b and, therefore, there is no gradient for a set of MUB. But the converse is not true: We can have a vanishing gradient although the bases are not pairwise unbiased.

When the gradient has nonzero components, we choose $\epsilon_a = \kappa G_a$ with a common $\kappa > 0$ that specifies the step size. This guarantees $\delta\overline{D^2} > 0$ if κ is not too large, and maximization along the line specified by the direction of the gradient can be done by optimizing the value of κ. The line optimization is a necessary ingredient if conjugate gradients are used for accelerating the convergence; see Ref. [28], for instance.

The finite unitary change of basis a, $|a_j\rangle \to V_a|a_j\rangle$, is then accomplished by

$$V_a = e^{i\epsilon_a}, \quad \text{or} \quad V_a = \frac{\mathbf{1}+i\epsilon_a/2}{\mathbf{1}-i\epsilon_a/2},$$
$$\text{or} \quad V_a = (\mathbf{1}+i\epsilon_a)\prod_{n=0}^{\infty}\left[\mathbf{1}+e^{i2\pi/3}\left(\epsilon_a^2\right)^{3^n}\right], \tag{A11}$$

or yet other ones, whichever of them is convenient to use. All three V_a equal $\mathbf{1}+i\epsilon_a$ to first order in ϵ_a and differ in the higher-order terms. Note that a high-precision evaluation of the infinite product in the third version of V_a requires very few terms. This makes the third version a viable alternative if the computation of the exponential in the first version or of the inverse operator in the second version is time consuming or imprecise.

The iteration is terminated when all components of the gradient vanish (in the numerical sense specified by the machine precision). We repeat this steepest-ascent search many times to ensure that we find the global maximum. As Fig. 1 shows for $(d,k) = (6,4)$, the iteration gets stuck in local maxima for about three attempts in ten; and, see Table I, only four in ten trials are successful for $(d,k) = (6,7)$.

APPENDIX B: DERIVATION OF THE TWO-PARAMETER FAMILY

The $d\times d$ matrix U_{ab} composed of the transition amplitudes $\langle a_j|b_k\rangle$ of two orthonormal bases is unitary,

$$U_{ab} = \begin{bmatrix}\langle a_1|\\ \langle a_2|\\ \vdots\\ \langle a_d|\end{bmatrix}[|b_1\rangle,|b_2\rangle,\ldots,|b_d\rangle] = U_{ba}^\dagger\,,$$
$$U_{ab}U_{ba} = \mathbb{1}\,. \tag{B1}$$

The columns and the rows of U_{ab} are representations of the kets $|b_k\rangle$ and the bras $\langle a_j|$, respectively. The unitary matrices associated with a set of bases have a composition law for consecutive basis changes: $U_{ab} = U_{ac}U_{cb}$, $U_{aa} = \mathbb{1}$. In particular, $\sqrt{d}\,U_{ab}$ is a complex Hadamard matrix if the bases a and b are unbiased; see the paragraph containing Eq. (4).

Now, from the numerical search we know that one of the bases that maximize the ASD between four bases in six dimensions is unbiased with the other three bases. We identify this privileged basis as the canonical basis and refer to it as the zeroth basis, and we characterize the set of four bases by the

three 6×6 transition matrices

$$M_1 = U_{01}\,, \quad M_2 = U_{02}\,, \quad M_3 = U_{03}\,, \tag{B2}$$

so that the columns of M_i are composed of the probability amplitudes of the kets of the ith basis with respect to the privileged basis.

When multiplied by $\sqrt{6}$, the matrices M_1, M_2, and M_3 are 6×6 Hadamard matrices, for which we use Karlsson's parametrization [25]. His parametrization applies to H_2-reducible Hadamard matrices that can be written in the form $H = X_L P_L N P_R X_R$, where the left and right X matrices only contain phases on the diagonal, the P matrices are permutation matrices, and the central matrix has the form

$$N = \begin{bmatrix} F_2 & T_1 & T_2 \\ T_3 & \frac{1}{2}T_3 A T_1 & \frac{1}{2}T_3 B T_2 \\ T_4 & \frac{1}{2}T_4 B T_1 & \frac{1}{2}T_4 A T_2 \end{bmatrix}, \tag{B3}$$

where F_2 is the unnormalized two-dimensional Fourier matrix of Eqs. (5) and the 2×2 matrices T_i are those of Eq. (16),

$$T_i = \begin{bmatrix} 1 & t_i \\ 1 & -t_i \end{bmatrix} \quad \text{with} \quad |t_i| = 1\,, \tag{B4}$$

while

$$\begin{aligned} A &= F_2\left(-\frac{1}{2}\mathbb{1} + i\frac{\sqrt{3}}{2}\Lambda\right), \\ B &= F_2\left(-\frac{1}{2}\mathbb{1} - i\frac{\sqrt{3}}{2}\Lambda\right), \end{aligned} \tag{B5}$$

with a unitary and Hermitian 2×2 matrix Λ. It turns out that our Hadamard matrices are indeed H_2 reducible since they can be written as $M_i = X_{L_i} P_{L_i} N_i P_{R_i} X_{R_i}$ with the central matrices given by

$$\begin{aligned} N_1 &= \frac{1}{\sqrt{6}}\begin{bmatrix} F_2 & F_2 & F_2 \\ F_2 & \omega F_2 & \omega^* F_2 \\ T & \omega^* T & \omega T \end{bmatrix}, \\ N_2 &= \frac{1}{\sqrt{6}}\begin{bmatrix} F_2 & F_2 & F_2 \\ T & \omega T & \omega^* T \\ T & \omega^* T & \omega T \end{bmatrix}, \\ N_3 &= \frac{1}{\sqrt{6}}\begin{bmatrix} F_2 & F_2 & F_2 \\ T & \omega T & \omega^* T \\ F_2 & \omega^* F_2 & \omega F_2 \end{bmatrix}; \end{aligned} \tag{B6}$$

see Eqs. (6).

As in Eqs. (5), we choose to express the matrix T with factors of $\omega = \exp(i2\pi/3)$,

$$T = \begin{bmatrix} 1 & \omega t^2 \\ 1 & -\omega t^2 \end{bmatrix}, \tag{B7}$$

to exhibit the crucial dependence on the phase factor t. The left permutation matrices are all equal, $P_{L_1} = P_{L_2} = P_{L_3} = P_L$.

Third, we notice that only the left dephasing and permutation matrices are relevant for the distance. Indeed the right dephasing matrices only add global phases to the basis vectors, while the right permutation only permutes the basis vectors. In other words, two bases B and $B P_R X_R$ are equivalent in terms of distance. Therefore we can choose to conserve only the relevant structure for our bases, that is, $M_i = X_{L_i} P_{L_i} N_i$.

The fourth step is to use the fact that only relative dephasing and permutations of the rows are relevant to the distance. Therefore we define new bases as

$$\begin{aligned} M_1 &\mathrel{\widehat{=}} P_L^\dagger X_2^\dagger X_1 P_L N_1\,, \\ M_2 &\mathrel{\widehat{=}} N_2\,, \\ M_3 &\mathrel{\widehat{=}} P_L^\dagger X_2^\dagger X_3 P_L N_3\,. \end{aligned} \tag{B8}$$

To simplify the notation, we again denote the two new diagonal matrices in $P_L^\dagger X_2^\dagger X_1 P_L$ and $P_L^\dagger X_2^\dagger X_3 P_L$ by X_1 and X_3, respectively. We further observe that

$$X_1 = \begin{bmatrix} A_1 & \mathbf{0} & \mathbf{0} \\ \mathbf{0} & A_2 & \mathbf{0} \\ \mathbf{0} & \mathbf{0} & A_1 \end{bmatrix}, \quad X_3 = \begin{bmatrix} B_1 & \mathbf{0} & \mathbf{0} \\ \mathbf{0} & B_2 & \mathbf{0} \\ \mathbf{0} & \mathbf{0} & B_3 \end{bmatrix}. \tag{B9}$$

Next we add a suitable global phase to X_1 and X_3. We multiply X_1 by $\exp[-i\,\mathrm{Arg}(A_1[1,1]A_1[2,2]/2)]$ and X_3 by $\exp[-i\,\mathrm{Arg}(B_1[1,1]B_1[2,2]/2)]$ such that A_1 and B_1 take the simple form

$$\begin{bmatrix} \exp(-i\phi) & 0 \\ 0 & \exp(i\phi) \end{bmatrix}, \tag{B10}$$

for some phase ϕ. We end up with the remarkable form

$$X_1 = \begin{bmatrix} A_1 & \mathbf{0} & \mathbf{0} \\ \mathbf{0} & A_2 & \mathbf{0} \\ \mathbf{0} & \mathbf{0} & A_1 \end{bmatrix}, \quad X_3 = \begin{bmatrix} A_1^* & \mathbf{0} & \mathbf{0} \\ \mathbf{0} & \omega^* A_1^* & \mathbf{0} \\ \mathbf{0} & \mathbf{0} & B_3 \end{bmatrix}, \tag{B11}$$

where [cf. Eqs. (5)]

$$A_1 = \begin{bmatrix} x^* & 0 \\ 0 & x \end{bmatrix}. \tag{B12}$$

So far, we have found that

$$\begin{aligned} A_3 &= A_1, \\ B_1 &= A_1^*, \\ B_2 &= \omega^* A_1^*, \end{aligned} \tag{B13}$$

and it only remains to find the structure behind the two 2×2 dephasing matrices A_2 and B_3.

To do so, we now consider the products $U_{ij} = M_i^\dagger M_j$. We obtain

$$M_1^\dagger M_2 = \begin{bmatrix} a_1 & a_2 & a_3 \\ a_3 & a_1 & a_2 \\ a_2 & a_3 & a_1 \end{bmatrix} \quad \text{with} \quad \begin{bmatrix} a_1 \\ a_2 \\ a_3 \end{bmatrix} = F_3 \begin{bmatrix} F_2 A_1^* F_2 \\ F_2 A_2^* T \\ T^\dagger A_3^* T \end{bmatrix}, \tag{B14}$$

and F_3 is the standard (unnormalized) three-dimensional Fourier matrix

$$F_3 = \begin{bmatrix} 1 & 1 & 1 \\ 1 & \omega & \omega^* \\ 1 & \omega^* & \omega \end{bmatrix}. \tag{B15}$$

Similarly we have

$$M_2^\dagger M_3 = \begin{bmatrix} b_1 & b_2 & b_3 \\ b_3 & b_1 & b_2 \\ b_2 & b_3 & b_1 \end{bmatrix} \quad \text{with} \quad \begin{bmatrix} b_1 \\ b_2 \\ b_3 \end{bmatrix} = F_3 \begin{bmatrix} F_2 B_1 F_2 \\ T^\dagger B_2 T \\ T^\dagger B_3 F_2 \end{bmatrix}, \tag{B16}$$

and

$$M_3^\dagger M_1 = \begin{bmatrix} c_1 & c_2 & c_3 \\ c_3 & c_1 & c_2 \\ c_2 & c_3 & c_1 \end{bmatrix} \quad \text{with} \quad \begin{bmatrix} c_1 \\ c_2 \\ c_3 \end{bmatrix} = F_3 \begin{bmatrix} F_2 Y_1 F_2 \\ T^\dagger Y_2 F_2 \\ F_2 Y_3 T \end{bmatrix}, \tag{B17}$$

where

$$Y = X_3^* X_1 = \begin{bmatrix} Y_1 & \mathbf{0} & \mathbf{0} \\ \mathbf{0} & Y_2 & \mathbf{0} \\ \mathbf{0} & \mathbf{0} & Y_3 \end{bmatrix} = \begin{bmatrix} A_1^2 & \mathbf{0} & \mathbf{0} \\ \mathbf{0} & \omega A_1 A_2 & \mathbf{0} \\ \mathbf{0} & \mathbf{0} & B_3^* A_1 \end{bmatrix}. \tag{B18}$$

The seventh step is to look once more at the numerics. With respect to the product $M_1^\dagger M_2$, we see that

$$a_2 = \omega^* Z a_3 Z\,. \tag{B19}$$

Thus we are led to define the matrix equation

$$E_1 \mathrel{\widehat{=}} a_2 - \omega^* Z a_3 Z = 0\,. \tag{B20}$$

This only represents a system of three equations since $E_1[1,1] = E_1[2,2]$. In the same manner, we have for $M_2^\dagger M_3$

$$E_2 \mathrel{\widehat{=}} b_1 - \omega^* Z b_3 Z = 0\,, \tag{B21}$$

and $E_2[1,1] = E_2[2,2]$, so that, here too, only three equations are relevant. Finally, for $M_3^\dagger M_1$, we obtain

$$E_3 \mathrel{\widehat{=}} c_1 + Z c_2 Z = 0, \tag{B22}$$

and, owing to $(\omega^* - 1)E_3[1,2] = t(1-\omega)E_3[2,1]$, again only three equations are relevant. We should mention here that there are other interesting identities within the products $M_i^\dagger M_j$, such as $b_2 = [a_1 + a_1^\dagger + Z(a_1 - a_1^\dagger)Z]/2$, but they are much more complicated to handle and will not be necessary to achieve our parametrization.

The eighth step is to solve the above nine equations. We obtain

$$\begin{aligned} &E_1[1,1]: \ \mathrm{tr}\{A_1\} = \mathrm{tr}\{A_3\}\,, \\ &E_1[1,2]: \ A_1 - 2\omega^* t^{*2} A_2 + \omega^* t^{*2} A_3 = r\mathbb{1}\,, \\ &E_1[2,1]: \ \omega^* t^{*2} A_1 - 2\omega^* t^{*2} A_2 + A_3 = r'\mathbb{1}\,. \end{aligned} \tag{B23}$$

From the numerics, we know that $r = r'$ and thus $A_1 = A_3$, which we already found by looking at the dephasing matrix X_1. Note also that the expression of the complex number r is not required. Furthermore we find

$$\begin{aligned} &E_2[1,1]: \ \mathrm{tr}\{B_1\} = \omega \mathrm{tr}\{B_2\}\,, \\ &E_2[1,2]: \ \omega^* t^{*2} B_1 + \omega B_2 - 2\omega t^{*2} A_3 = s\mathbb{1}\,, \\ &E_2[2,1]: \ B_1 + t^{*2} B_2 - 2\omega t^{*2} B_3 = s'\mathbb{1}\,. \end{aligned} \tag{B24}$$

From the numerics, we know that $s = s'(= r)$ and thus $B_1 = \omega B_2$, which we already obtained by looking at the dephasing matrix X_3. The next three equations are much more interesting. Indeed we have

$$\begin{aligned} &E_3[1,1]: \ 2\mathrm{tr}\{Y_1\} - \omega^* \mathrm{tr}\{Y_2\} - \omega \mathrm{tr}\{Y_3\} = 0\,, \\ &E_3[2,2]: \ 2\mathrm{tr}\{Y_1\} - \omega t^{*2} \mathrm{tr}\{Y_2\} - \omega^* t^2 \mathrm{tr}\{Y_3\} = 0, \\ &E_3[1,2]: \ t^{*2} Y_2 - Y_3 = u\mathbb{1}. \end{aligned} \tag{B25}$$

From the numerics, we know that $u = 0$ and the last equation reduces to

$$Y_3 = t^{*2} Y_2. \tag{B26}$$

Since $Y_2 = \omega A_1 A_2$ and $Y_3 = B_3^* A_1$, the above equation directly translates into

$$B_3 = \omega^* t^2 A_2^*\,. \tag{B27}$$

This last relation can be inserted in $E_3[1,1]$ and $E_3[2,2]$, which become identical and can be written as

$$2\mathrm{tr}\{Y_1\} - (\omega^* + \omega t^{*2})\mathrm{tr}\{Y_2\} = 0\,. \tag{B28}$$

This equation will soon become Eq. (7).

A last hint from the numerics is needed. We actually notice that

$$Y_1 Y_2 Y_3 = -\mathbb{1}\,. \tag{B29}$$

As $Y_3 = t^{*2} Y_2$, we arrive at $t^{*2} Y_1 Y_2^2 = -\mathbb{1}$ so that $\omega t^* A_1^2 A_2 = \pm i U$, where $U^2 = \mathbb{1}$, that is, $U = \mathbb{1}$ or $U = Z$ since it has to be diagonal. With the help of the numerics, we conclude that

$$A_2 = i\omega^* t Z A_1^{*2}, \tag{B30}$$

and consequently

$$B_3 = -it Z A_1^2\,. \tag{B31}$$

The final parametrization of the dephasing matrices is therefore given by

$$\begin{aligned} X_1 &= \begin{bmatrix} A_1 & \mathbf{0} & \mathbf{0} \\ \mathbf{0} & i\omega^* t Z A_1^{*2} & \mathbf{0} \\ \mathbf{0} & \mathbf{0} & A_1 \end{bmatrix}, \\ X_3 &= \begin{bmatrix} A_1^* & \mathbf{0} & \mathbf{0} \\ \mathbf{0} & \omega^* A_1^* & \mathbf{0} \\ \mathbf{0} & \mathbf{0} & -it Z A_1^2 \end{bmatrix}, \end{aligned} \tag{B32}$$

which are ingredients in Eqs. (6).

Let us finally come back to Eq. (B28). We can now substitute $Y_1 = A_1^2$ and $Y_2 = (i\omega^* t Z A_1^{*2})(\omega A_1) = it Z A_1^*$ in Eq. (B28) and, upon defining $x = \exp(i\theta_x)$ and $t = \exp(i\theta_t)$, we arrive at

$$\cos(\theta_t - 2\pi/3) = -\frac{\cos(2\theta_x)}{\sin(\theta_x)}\,, \tag{B33}$$

which is Eq. (7).

[1] H. Weyl, Z. Phys. **46**, 1 (1927).
[2] J. Schwinger, Proc. Nat. Acad. Sci. **46**, 570 (1960).
[3] N. Bohr, Naturwissenschaften **16**, 245 (1928); Nature (London) **121**, 580 (1928).
[4] M. O. Scully, B.-G. Englert, and H. Walther, Nature (London) **351**, 111 (1991).
[5] J. Schwinger, *Quantum Mechanics—Symbolism of Atomic Measurements* (Springer-Verlag, Berlin, 2003).
[6] B.-G. Englert, *Lectures on Quantum Mechanics—Perturbed Evolution* (World Scientific, Singapore, 2006).
[7] T. Durt, B.-G. Englert, I. Bengtsson, and K. Życzkowski, Int. J. Quant. Inform. **8**, 535 (2010).
[8] I. D. Ivanovic, J. Phys. A **14**, 3241 (1981).
[9] W. K. Wootters and B. D. Fields, Ann. Phys. (NY) **191**, 363 (1989).
[10] B.-G. Englert, D. Kaszlikowski, L. C. Kwek, and W. H. Chee, Int. J. Quant. Inform. **6**, 129 (2008).
[11] N. J. Cerf, M. Bourennane, A. Karlsson, and N. Gisin, Phys. Rev. Lett. **88**, 127902 (2002).
[12] T. Durt, e-print arXiv:quant-ph/0401046.
[13] A. B. Klimov, D. Sych, L. L. Sanchez-Soto, and G. Leuchs, Phys. Rev. A **79**, 052101 (2009).
[14] M. Revzen, Phys. Rev. A **81**, 012113 (2010).
[15] S. Bandyopadhyay, P. O. Boykin, V. Roychowdhury, and F. Vatan, Algorithmica **34**, 512 (2002).
[16] A. Klappenecker and M. Rötteler, Lect. Notes Comput. Sci. **2948**, 262 (2004).
[17] T. Durt, J. Phys. A **38**, 5267 (2005).
[18] G. Zauner, Int. J. Quant. Inform. **9**, 445 (2011).
[19] M. Grassl, e-print arXiv:quant-ph/0406175.
[20] S. Brierley and S. Weigert, Phys. Rev. A **78**, 042312 (2008).
[21] S. Brierley and S. Weigert, J. Phys. Conf. Ser. **254**, 012008 (2010).
[22] I. Bengtsson, W. Bruzda, Å. Ericsson, J.-Å. Larsson, W. Tadej, and K. Życzkowski, J. Math. Phys. **48**, 052106 (2007).
[23] P. Butterley and W. Hall, Phys. Lett. A **369**, 5 (2007).
[24] M. J. Hadamard, Bull. Sci. Math. **17**, 24 (1893).
[25] B. R. Karlsson, Lin. Alg. Appl. **434**, 239 (2011).
[26] U. Haagerup, in *Operator Algebras and Quantum Field Theory (Rome)* (International Press, Cambridge, MA, 1996), p. 296.
[27] P. Jaming, M. Matolsci, P. Móra, F. Szöllősi, and M. Weiner, J. Phys. A **42**, 245305 (2009).
[28] J. R. Shewchuck, An Introduction to the Conjugate Gradient Method Without the Agonizing Pain Edition $1\frac{1}{4}$, available at [http://www.cs.cmu.edu/∼quake-papers/painless-conjugate-gradient.pdf].